

The Spin Reorientation Transition and Phase Diagram of Ultrathin Ferromagnetic Films

Marianela Carubelli,^{1,*} Orlando V. Billoni,^{1,†} Santiago Pighín,^{1,‡} Sergio A. Cannas,^{1,§} Daniel A. Stariolo,^{2,¶} and Francisco A. Tamarit^{1,**}

¹*Facultad de Matemática, Astronomía y Física, Universidad Nacional de Córdoba, Ciudad Universitaria, 5000 Córdoba, Argentina*^{††}

²*Departamento de Física, Universidade Federal do Rio Grande do Sul CP 15051, 91501-979, Porto Alegre, Brazil*^{‡‡}

(Dated: February 2, 2008)

We show results from Monte Carlo simulations of a two dimensional Heisenberg model for ultrathin films with perpendicular anisotropy. A complete phase diagram is obtained as a function of anisotropy and temperature, spanning a wide range of behavior. We discuss our results in relation with experimental findings in different ultrathin films. We observe and characterize a line of Spin Reorientation Transitions. This transition from out of plane stripe order to in plane ferromagnetic order presents a paramagnetic gap in between in a finite region in parameter space, as reported in experiments. For large anisotropies direct transitions from a low temperature stripe phase to a paramagnetic or tetragonal phase with dominant perpendicular magnetization is observed, also in agreement with experiments.

We also show the phase diagram for a system without exchange, i.e. with pure dipolar and anisotropy interactions. It shows a similar behavior to the ferromagnetic case with antiferromagnetic instead of stripe phases at low temperatures. A Spin Reorientation Transition is also found in this case.

PACS numbers: 75.40.Gb, 75.40.Mg, 75.10.Hk

Keywords: Monte Carlo simulations, Heisenberg model, ultrathin films, spin reorientation transition

I. INTRODUCTION

In recent years magnetic behavior of ultrathin films has become of great technological importance due to the applications in magnetic storage devices. As the sizes become smaller and smaller a detailed microscopic characterization of magnetization processes on the nanometer scale is mandatory. Magnetic order in ultrathin ferromagnetic films is very complex due to the competition between exchange and dipolar interactions on different length scales, together with a strong influence of shape and magnetocrystalline anisotropies of the sample. These in turn are very susceptible to the growth conditions of the films¹. In the last 20 years a considerable amount of experimental results on different aspects of magnetism in ultrathin films have appeared. Nevertheless, after a careful analysis of the literature it is difficult to reach general conclusions even in seemingly basic things as the kind of magnetic order at low temperatures. In view of this complexity, theoretical work on simplified models and computer simulations are essential for rationalizing and guiding new experimental work. In early experiments on Fe/Cu(100) films, Pappas *et al.*² and Allenspach *et al.*³ observed a spin reorientation transition (SRT) from a region with perpendicular magnetization to one with in-plane magnetization. In the first experiment Pappas *et al.* found a gap with a complete loss of magnetization in between the perpendicular and in-plane phases. Two hypothesis were put forward for the origin of the gap: a dynamic origin due the compensation of perpendicular and in-plane anisotropies in the region around the SRT and a static one based on previous theoretical work by Yafet *et al.*⁴ who predicted a striped magnetic phase as the true ground state of ultrathin films with perpendicular anisotropy. In the second experiment Allenspach *et al.* discarded the possibility of a completely vanishing magnetization in the vicinity of the SRT,

but instead observed the emergence of stripe magnetic order with a temperature dependent stripe width in general agreement with Yafet predictions. In their measurements no gap was observed between the perpendicular and in-plane phases. We will show that in fact this kind of behavior, with a direct SRT from a striped to a ferromagnetic in-plane state, is present in a particular anisotropy-temperature region in the phase diagram of our model. Furthermore, the thickness dependence of the SRT temperature observed by Pappas *et al.* can be qualitatively reproduced by our results on a single monolayer, after noting that the anisotropy behaves as the inverse of the film thickness, as discussed below.

More recently Won *et al.*⁵ studied the SRT as a function of temperature and thickness in Fe/Ni/Cu(001) films. They found an exponential decrease of stripe width on approaching the SRT and the possibility of a paramagnetic gap between the out of plane stripe phase and the in-plane ferromagnetic phase. The existence of the gap was interpreted by the authors in terms of a crossover between typical dipolar and anisotropy lengths. They defined a Curie temperature as a function of the dipolar length and depending on it being higher or lower than the SRT temperature, a paramagnetic gap may or may not manifest in the system. Indeed, we will show that also this kind of behavior with a SRT and a gap is present in a particular anisotropy-temperature region in the phase diagram of our model. Although we were not able to test quantitatively the phenomenological arguments of Won *et al.* because of our too small working stripe width, their conclusions are completely consistent with the scenario that emerges from our simulations. In yet another set of important experiments Vaterlaus *et al.*⁶ found evidence of a two step disordering process. The films show stripe phases at low temperatures which loose orientational order and eventually evolve into a “tetragonal liquid phase” with short range stripe order showing 90° rotational

symmetry. This phase further evolves in a continuous way towards a final paramagnetic phase. In these experiments the films present strong perpendicular anisotropy and no SRT is observed; magnetization is always out of plane. We will show that this is also observed in our simulations in the parameter region corresponding to strong anisotropy. In this region of the phase diagram a direct transition from a stripe phase to a paramagnetic (or tetragonal) phase is observed. In the region of strong anisotropy the thermodynamic phases can be studied in the Ising limit. Detailed ground state calculations⁷ and numerical simulations^{8,9,10} have been done in recent years and a successful picture of this region of the phase diagram has emerged. In an extended region of temperatures and anisotropies MacIsaac *et al.*¹¹ have presented a phase diagram of an Heisenberg model with dipolar and exchanged interactions. Their phase diagram (figure 3 of their letter) is similar to our present results. Nevertheless both diagrams differ in an important result: while they obtained a SRT from a low temperature perpendicular stripe phase to an in-plane ferromagnet at higher temperatures (at variance with most experiments), our results show the inverse trend, *i.e.*, from an in-plane ferromagnet at low temperature to perpendicular a stripe or paramagnetic phase at high temperatures, consistent with experimental results. Our SRT line is supported by experimental as well as several theoretical arguments as will be explained below.

The nature of the different phase transitions is a delicate issue and several controversial results are spread in the literature. In the present work we did not pursue to set in a definitive answer, but nevertheless we added new results to the old ones. In the high anisotropy limit our results regarding the nature of the stripe-tetragonal phase are again consistent with similar simulations in Ising systems which point to predominantly first order transitions. This result is again at variance with the

continuous transition reported by MacIsaac *et al.* on the same region¹¹. At intermediate anisotropies the same transition line gradually changes its behavior and the transition seems to become continuous or weakly first order in the region where a gap is observed around the SRT. This behavior is similar to the phenomenology observed recently in field theoretical models for thin films with Langevin dynamics^{12,13}. Another relevant aspect concerns the possible existence of an intermediate nematic phase as predicted theoretically by Abanov *et al.*¹⁴ and recently on more general grounds by Barci *et al.*¹³ and characterized in Langevin simulations by Nicolao *et al.*¹² and also in Monte Carlo simulation of an Ising model by Cannas *et al.*⁹. In the rest of this work we will refer to stripe phases regardless of the existence of true long range positional order or only orientational order. Besides the stripes-tetragonal or paramagnetic transition line, we obtained convincing evidence for a first order nature of the SRT line and the continuous nature of the in-plane ferromagnetic-paramagnetic transition, as will be shown below.

Finally we also show a complete phase diagram of the pure dipolar system with perpendicular uniaxial anisotropy. The phase diagram in this limit is similar to the one with exchange interaction, the main difference being the small slope of the SRT line as compared to the ferromagnetic case and the anti-ferromagnetic nature of the low temperatures phases.

II. MODEL AND METHODS

We have performed Monte Carlo (MC) simulations on the usual model Hamiltonian for ultrathin films with exchange, dipolar and perpendicular anisotropy on a square lattice of side $L = 40$:

$$\mathcal{H} = -\delta \sum_{\langle i,j \rangle} \vec{S}_i \cdot \vec{S}_j + \sum_{(i,j)} \left[\frac{\vec{S}_i \cdot \vec{S}_j}{r_{ij}^3} - 3 \frac{(\vec{S}_i \cdot \vec{r}_{ij})(\vec{S}_j \cdot \vec{r}_{ij})}{r_{ij}^5} \right] - \eta \sum_i (S_i^z)^2 \quad (1)$$

where the exchange and anisotropy constants are normalized relative to the dipolar coupling constant, $\langle i,j \rangle$ stands for a sum over nearest neighbors pairs of sites in the lattice, (i,j) stands for a sum over *all distinct* pairs and $r_{ij} \equiv |\vec{r}_i - \vec{r}_j|$ is the distance between spins i and j . All the simulations were done using the Metropolis algorithm and periodic boundary conditions were imposed on the lattice by means of the Ewald sums technique. All the results presented in section III refer to the case $\delta = 3$ which corresponds, for large values of η , to a ground state with out of plane stripe magnetic structure of width⁷ $h = 4$ and to an in-plane ferromagnetic ground state for small anisotropy (see figure 1).

Each spin is defined by a unit vector with components S^x, S^y, S^z . The phase diagram has been obtained measuring

the out plane magnetization:

$$M_z \equiv \frac{1}{N} \sum_{\vec{r}} \langle S^z(\vec{r}) \rangle, \quad (2)$$

the in-plane magnetization:

$$M^{\parallel} \equiv \sqrt{(M^x)^2 + (M^y)^2}, \quad (3)$$

and an orientational order parameter similar to the one defined by Booth *et al.*¹⁵:

$$O_{hv} \equiv \left\langle \left| \frac{n_h - n_v}{n_h + n_v} \right| \right\rangle \quad (4)$$

where $\langle \dots \rangle$ stands for a thermal average, n_h (n_v) is the number of horizontal (vertical) pairs of nearest neighbor spins with

antialigned perpendicular component, *i.e.*,

$$n_h = \frac{1}{2} \sum_{\vec{r}} \{1 - \text{sig}[S^z(r_x, r_y), S^z(r_x + 1, r_y)]\} \quad (5)$$

and a similar definition for n_v , where $\text{sig}(x, y)$ is the sign of the product of x and y . In the previous definitions $N = L \times L$ is the number of spins and M^x, M^y are defined similarly to equation (2). Other quantities calculated were the specific heat

$$C \equiv \frac{1}{NT^2} \left(\langle H^2 \rangle - \langle H \rangle^2 \right) \quad (6)$$

and the mean absolute magnetization

$$P \equiv \frac{1}{N} \sum_{\vec{r}} \langle |S^z(\vec{r})| \rangle \quad (7)$$

In section IV we calculate the phase diagram for $\delta = 0$ (dipolar interactions plus anisotropy). In this case the relevant phases at low temperatures are antiferromagnetic (AF). For high values of the anisotropy the ground state is AF with sub-lattice magnetization and all the spins oriented perpendicular to the plane¹⁶. For low values of the anisotropy the ground state is a highly degenerated planar AF state; the different configurations of this state are described in Ref.¹⁷. To characterize the perpendicular AF state we calculated the staggered perpendicular magnetization

$$M_{s\perp} \equiv \frac{1}{N} \left\langle \left| \sum_{\vec{r}} (-1)^{r_x+r_y} S^z(\vec{r}) \right| \right\rangle \quad (8)$$

To characterize the planar AF state we calculated the following orientational order parameter^{16,17}

$$M_{s\parallel} \equiv \frac{1}{N} \left\langle \left| \sum_{\vec{r}} (-1)^{r_y} S^x(\vec{r}) \hat{x} + (-1)^{r_x} S^y(\vec{r}) \hat{y} \right| \right\rangle \quad (9)$$

To obtain the phase diagrams T vs η we analyzed the behavior of the above quantities by fixing η and varying T or viceversa. Those curves were calculated using two different simulation protocols.

To analyze equilibrium properties we use a ladder protocol, where the system is initialized at some configuration close to the equilibrium one (either the corresponding ground state at low temperatures or the paramagnetic one at high temperatures) and the independent parameter (η or T) is varied at discrete steps. The initial configuration for every value of the independent parameter was taken as the last one of the previous value; then we discarded the first t_e Monte Carlo Steps (MCS) needed for equilibration and calculated the averages over the next t_m MCS. A MCS is defined as a complete cycle of N spin update trials, according to the Metropolis algorithm. Typical values of t_e were around 10^5 MCS, while typical values of t_m were between 10^3 and 10^4 MCS.

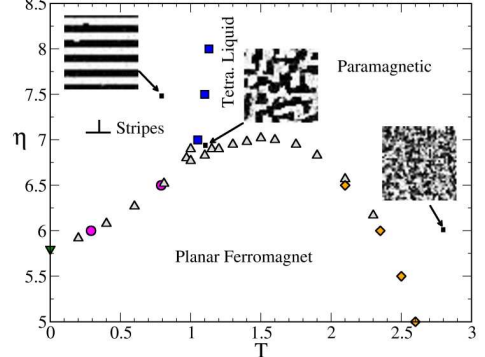


FIG. 1: (Color online) The phase diagram η vs. Temperature for $\delta = 3$. The different symbols corresponds to different calculation methods; triangle down (green): ground state calculation; circle (red): energy histograms simulations; square (blue): order parameter histogram simulations; triangle up (white): equilibrium and non-equilibrium order parameters simulations (see methods); diamond (yellow): specific heat simulations. Some typical spin configurations (perpendicular component of the spins) are shown at different phases

To analyze the possible existence of hysteresis effects we used a “cooling-heating” procedure, varying the temperature (or η) according to a linear protocol $T(t) = T(0) \pm r t$, where $T(0)$ is the initial temperature, t is measured in MCS and r is a constant rate. Before starting the protocol we let the system to equilibrate during t_e MCS from some appropriated initial configuration (as in the previous protocol) and then we recorded the quantities of interest as a function of time along a complete path to the final temperature; then we repeated the procedure several times, averaging the whole curves over different sets of initial configurations (in the cases were they are random) and over different sequences of thermal noise; typical sample sizes were between 50 and 100.

III. PHASE DIAGRAM FOR THE FERROMAGNETIC MONOLAYER

In figure 1 we show the phase diagram in the (η, T) plane. The different transition lines were obtained by measuring more than one quantity as is indicated in the figure with different symbols.

As can be seen all lines are smooth which gives confidence to the quality of the data. We can clearly distinguish three different phases: perpendicular stripes for low temperatures and strong anisotropy, in-plane ferromagnet for low temperatures and weak anisotropy and paramagnetic behavior for high temperatures. The disordering of the stripe phase with temperature evolves through a region where the orientational order is lost but a lower symmetry to 90° rotations survives and continuously evolves to the complete paramagnetic state. We will call this region *tetragonal phase* although there is no clear evidence that a sharp transition to a paramagnetic phase with full rotational symmetry is present at high temperatures.

A. Stripes-Tetragonal transition

In figure 1 we see that for $\eta > 7$ the system goes through a phase transition from a phase with perpendicular stripe order, with stripes of width $h = 4$ lattice spacings to a high temperature “tetragonal phase”. This transition line has been obtained calculating histograms of the order parameter O_{hv} . One such histogram for $\eta = 7.5$ and three characteristic temperatures is shown in figure 2. Clear evidence of a first order transition is given by the behavior of the histogram showing two metastable phases (stripes and tetragonal) changing stability around the transition temperature ($\approx T = 1.1$ in this case). This is at variance with results by MacIsaac *et al.*¹¹ who reported a line of second order transitions. The first order nature of this transitions for large anisotropies is in agreement with recent results for a corresponding Ising model with dipolar interactions⁸. Furthermore, as figure 1 shows, this line seems to go asymptotically for large η , to a value of the transition temperature $T \approx 1.2$ which is in good agreement with the phase diagram of the Ising model¹⁸. This quantitative agreement gives further credit to the first order nature of this transition line, at least for large η where the Ising approximation is justified. More or less direct experimental evidence for the appearance of stripes magnetic structures was reported already in an old work by Allenspach and Bischoff³. More recently the striped nature of the low temperature phase of high anisotropy, perpendicular Fe/Cu(100) films, together with the transition to a phase with tetragonal symmetry have been measured and confirmed by Vaterlaus *et al.*⁶. A theoretical model predicting the existence of a phase with 90° symmetry induced by the underlying symmetry of the lattice was put forward by Abanov *et al.*¹⁴. Abanov *et al.* theory works in the Ising limit where only the perpendicular component of the magnetization is relevant for the thermodynamic behavior. Their model admits two possible scenarios for the disordering of the stripes: one similar to the present results with a first order transition from a stripe phase with positional order decaying algebraically with distance to a paramagnetic phase with a residual 90° symmetry, and a second possibility, depending on the values of elastic constants of the theory, in which an intermediate nematic phase appears between the stripes and paramagnetic phases. Furthermore, the perpendicular tetragonal phase can evolve continuously to a full paramagnetic phase or it can finish at a spin reorientation transition. Interestingly, our phase diagram shows these two behaviors (see figure 1): for an interval $6.7 \leq \eta \leq 7$ the Heisenberg system goes from stripes to tetragonal and then to a planar ferromagnet through a SRT. At still higher temperatures the in-plane ferromagnet disorders via a continuous transition. This kind of behavior was already reported in experiments on Fe/Cu(100) ultrathin films by Pappas *et al.*² who found a gap in magnetization between the perpendicular and planar phases (see figure 1 of Ref.²). Nevertheless, in that early experiments the nature of the gap was not clear and the authors pointed out two possibilities: a real paramagnetic gap or the fact that the width of the stripes (not seen in the experiment) could diminish rapidly in the region of the SRT. One must note that the perpendicular phase in that series of experiments referred to samples with finite mag-

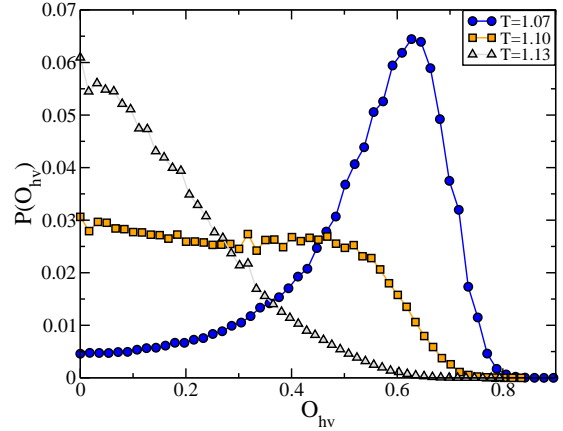


FIG. 2: (Color online) Order parameter O_{hv} per spin histograms for $\eta = 7.5$ and different temperatures. The histograms were calculated for 30×10^6 values of the energy, measured along a single MC run.

netization at low temperatures, not stripe order. Indeed, further experiments by Allenspach *et al.*³ confirmed the second hypothesis for the same range of thickness of Pappas *et al.*. More recently, Won *et al.*⁵ analyzed domain formation and the nature of the SRT in ultrathin films of Fe/Ni/Cu(001) using high resolution Photoemission Electron Microscopy imaging techniques. They observed both kind of behaviors, according to the film thickness range, namely, a direct SRT from the striped state and a transition mediated by a paramagnetic gap. In this case, the resolution of the experiment rules out the possibility of domains with a stripe width below the magnetic spatial resolution in the gap region. However, as the authors pointed out, the possibility of a fast-moving striped domain phase cannot be excluded in that experiment. Direct inspection of the typical spin configurations (see snapshot in figure 1) indicate that in our simulations the gap corresponds to an out-of-plane tetragonal phase appearing between the perpendicular stripe and planar ferromagnetic phases. Nevertheless, in experiments only temporal averages can be observed. To emulate the acquisition image process of the experiments, we calculated a time average of the local magnetization (perpendicular component)

$$\overline{m_\tau}(\vec{r}) \equiv \frac{1}{\tau} \sum_{t=1}^{\tau} S^z(\vec{r}, t) \quad (10)$$

for different values of the “acquisition time” τ , where all the times are measured in MCS. In figure 3 we show $\overline{m_\tau}(\vec{r})$ at three different values of τ in the striped and tetragonal liquid phases. The loss of contrast in the tetragonal liquid phase for relatively short times τ shows that the characteristic time scales for the fluctuations in this phase are much shorter than in the striped phase.

In figure 4 we show the orientational order parameter O_{hv} and in-plane magnetization M^{\parallel} for $\eta = 6.9$ as a function of

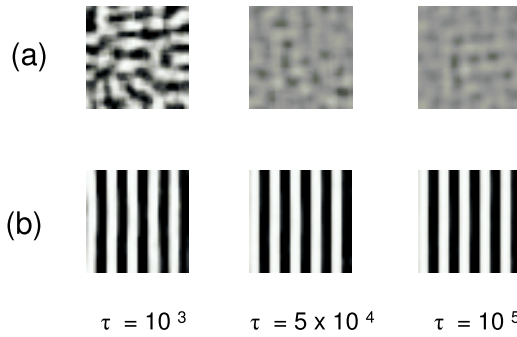


FIG. 3: Time average of the local perpendicular magnetization $\overline{m}_\tau(\vec{r})$ at different average times τ (all times are measured in MCS) for $\delta = 3$, $\eta = 6.9$ and $L = 40$. Before calculating $\overline{m}_\tau(\vec{r})$ the system was thermalized during $t = 10^5$ MCS at each temperature. (a) $T = 1.1$ (tetragonal liquid phase); (b) $T = 0.9$ (striped phase).

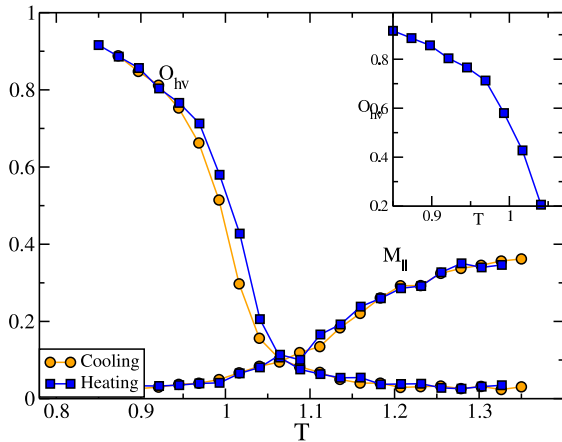


FIG. 4: (Color online) Order parameter O_{hv} and in plane magnetization $M_{||}$ as a function of temperature for $\delta = 3$, $\eta = 6.9$. The system was first thermalized at $T = 1.4$ and cooled with a rate $r = 10^{-7}$ and then heated again with the same rate. The error bars are of the same order of the symbol size. The inset shows a zoom of the heating curve

temperature. Figure 4 was obtained by performing cooling and heating cycles at a very small cooling rate $r = 10^{-7}$. Note that the stripe-tetragonal transition shows weak hysteresis. This indicates that the transition may be weakly first order or even continuous in this region. For giving a definite answer one must simulate larger samples and obtain much better statistics. Nevertheless it is clear from these curves that the sharp first order transition present for higher values of the anisotropy is much weaker in this region. Notice also the presence of a small shoulder in the orientational order parameter (see inset of figure 4). This effect is more marked in many individual realizations of the stochastic noise, where an almost saturated value of O_{hv} smaller than one can be observed in a narrow range of temperatures below the transition one. The same effect appears for larger values of η . This opens the possibility for the second scenario predicted by Abanov *et al.*¹⁴ of an intermediate perpendicular nematic phase, with long

range orientational order but without positional order. Evidence for this phase comes also from simulations of the Ising dipolar model⁹ and a recent theoretical model for the nematic transition in two dimensional systems with competing interactions^{12,13}.

B. Spin Reorientation Transition

In the region between $\eta = 5.8$ and $\eta = 7.0$ we observe a sharp SRT directly from a perpendicular stripe phase to a planar ferromagnetic one. The behavior of the orientational order parameter and the in-plane magnetization with temperature is shown in figure 5. In this region the order parameter O_{hv} is

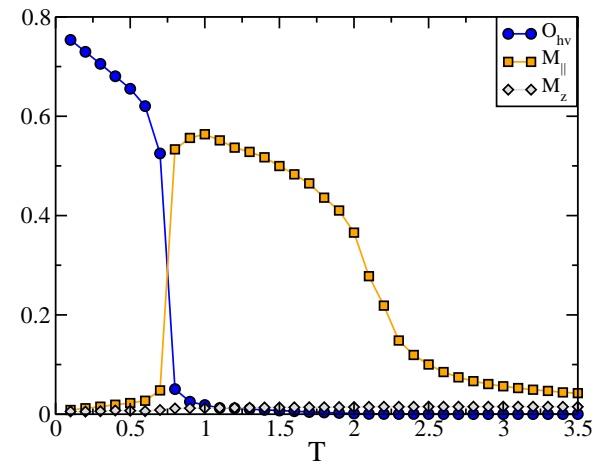


FIG. 5: (Color online) Order parameter O_{hv} , in plane and out of plane magnetizations $M_{||}$ and M_z as a function of temperature for $\delta = 3$ and $\eta = 6.5$. The system was initialized at infinite temperature, thermalized at $T = 6$ and then it was cooled (equilibrating at each temperature).

between the perpendicular and in-plane phases.

The SRT can be accessed both by varying the temperature in a film of fixed thickness or also by varying the thickness d of the film at fixed temperature. In fact, as the thickness grows the in-plane anisotropy induced by the dipolar interactions is reinforced, while the perpendicular anisotropy stays nearly constant due to its essentially surface character. Consequently at some thickness a SRT can be observed. Then, it is reasonable to consider a phenomenological model where the thickness acts equivalently to the inverse anisotropy: $d \propto 1/\eta$. In fact, Won *et al.*⁵ reported detailed measurements of magnetic changes as the thickness or temperature of samples of Fe/Ni/Cu(001) changed. They rationalized the observed behavior through a phenomenological model and summarized their findings in a phase diagram “temperature versus Fe thickness”, figure 5 of the cited paper. Assuming an approximate equivalence between thickness and inverse anisotropy, as

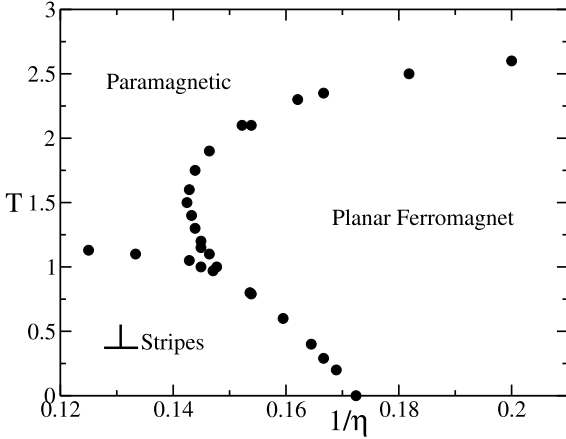


FIG. 6: Phase diagram temperature versus inverse anisotropy

explained above, we plotted our simulation data in a “ T versus $1/\eta$ ” diagram, as shown in figure 6. This figure shows a striking similarity with the right half of figure 5 of Won *et al.* reinforcing the equivalent character of film width and anisotropy in these systems.

The order of appearance of the perpendicular and planar phases is the main difference between our results and a previous phase diagram for the same model obtained by MacIsaac *et al.*¹¹. Those authors obtained a SRT line in the reverse order, from perpendicular at high temperatures to planar at low temperatures. As shown above, the correctness of our results is supported by experimental evidence on different ultrathin films as well as by theoretical analysis on the effect of thermal fluctuations on the SRT at fixed film thickness. Thermal fluctuations renormalize the dipolar and anisotropy coupling parameters in such a way that the anisotropy $K(T)$ diminishes faster than the dipolar coupling constant $g(T)$ ^{19,20} (in our notation $\eta = K/g$). Those works predict a linear dependence of the transition temperature $T_{SRT}(\eta)$ with anisotropy with positive slope, which is roughly in agreement with our SRT line from Monte Carlo simulations. In figure 7 we show cycles of O_{hv} and $M_{||}$ varying η at a fixed temperature of $T = 0.6$ in the SRT region. The cycles show a strong hysteretic behavior. This is further confirmed by means of energy histograms shown in figure 8 which show again the change in stability between the perpendicular and planar phases, a signature of the first order nature of the SRT, as predicted theoretically by several authors^{19,21}.

C. Planar Ferromagnetic-Paramagnetic Transition

This transition line shows a maximum around $\eta = 7$, $T = 1.5$ in the (η, T) plane. One can expect that the behavior of the system across the transition line will be different in the regions to the right and to the left of the maximum point. In the far right the system goes continuously from an in-plane ferromagnet to a paramagnetic phase. We have not been able to characterize completely the nature of this transi-

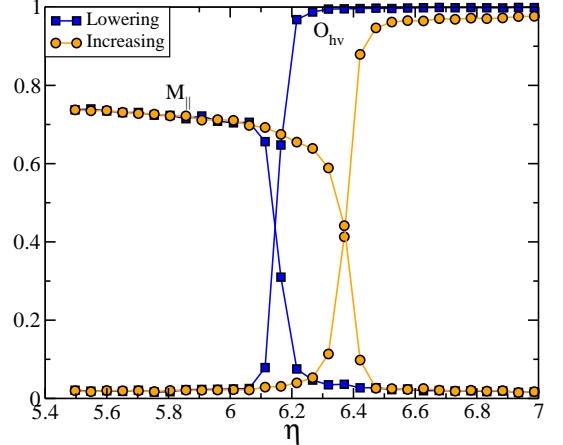


FIG. 7: (Color online) Order parameter O_{hv} and in plane magnetization $M_{||}$ as a function of η for $\delta = 3$ and $T = 0.6$. The system was initialized in stripes of with 4, thermalized at $\eta = 7.5$ and then η was lowered and then increased with a rate of $r = 10^{-5}$.

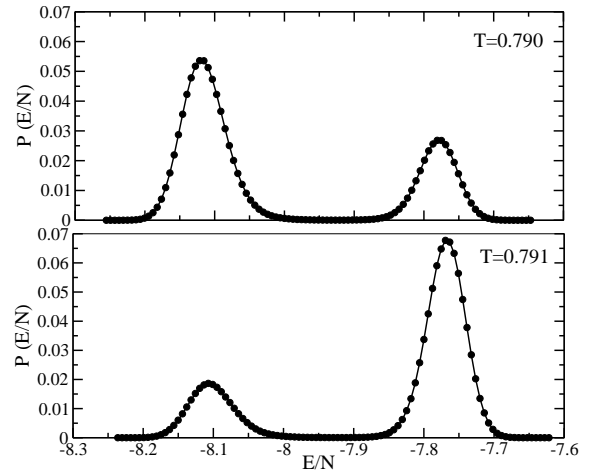


FIG. 8: Energy per spin histograms for $\delta = 3$, $\eta = 6.5$ and $T = 0.790$ (up) and $T = 0.791$ (down). The histograms were calculated for 30×10^6 energies measured along a single MC run.

tion, although our results appear to be consistent with a second order one.

In figure 9 we show that already at small values of η , deep in the planar phase, the spins have a finite perpendicular component, which grows continuously with η as the system goes through the phase transition. At some point around $\eta = 7$ the curves show an inflection point upon which the perpendicular component tends to saturate. This value of η drifts towards slightly smaller values as the temperature increases.

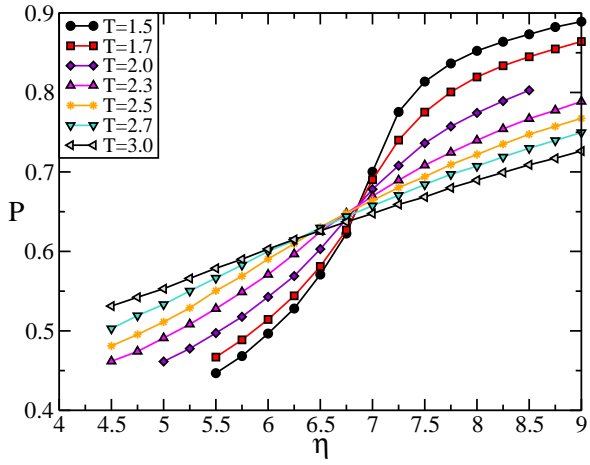


FIG. 9: (Color on line) Mean absolute magnetization P for different temperatures as function of η across the planar ferro-paramagnetic line ($\delta = 3$ and $L = 24$).

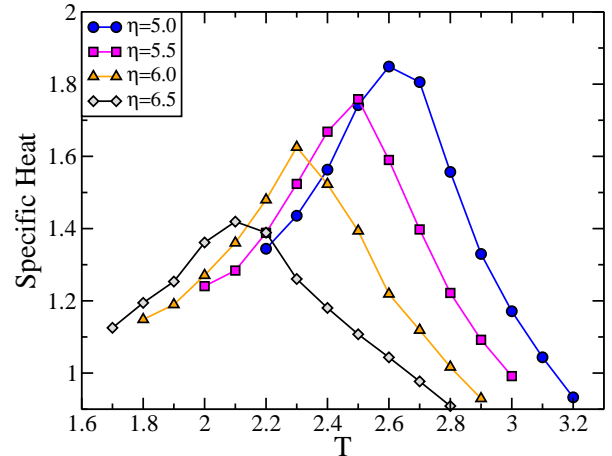


FIG. 10: (Color on line) Specific heat for $\delta = 3$ and different values of η .

We do not have a clear interpretation for the crossing points. It would be very interesting to analyze the domain walls in the paramagnetic phase and how they influence the evolution of the perpendicular magnetization as the system goes through the phase transition with finite in-plane magnetization. One may naively expect the perpendicular component of the local magnetizations m_i^z to vanish in this region, but this is not the case as figure 9 shows.

In figure 10 specific heat curves are shown for different anisotropies in the same region to the right of the maximum along the transition line. Note that the peak in the specific heat decreases as the transition approaches the maximum point from the right, suggesting a weakening of the second order character of the transition in this direction. In figure 11 we show an hysteresis cycle in η of the parallel component of the magnetization for a temperature to the left of the maximum point of the curve. A very weak hysteresis effect is observed. This behavior is compatible with a continuous transition or even a weakly first order one. Note that above the transition line in this region the system enters the tetragonal phase as discussed above. This phase has a different symmetry as compared with the paramagnetic high temperature phase. The change from the continuous rotational symmetry of the planar ferromagnetic phase to the discrete rotational symmetry of the tetragonal liquid would be compatible with a discontinuous phase transition in that part of the phase diagram. Also notice that actually along this line there is also a SRT, because the tetragonal liquid phase is perpendicularly oriented. Since we already showed the first order nature of the SRT at planar ferromagnetic-striped transition line (where a similar change of symmetry happens), one would expect the planar ferromagnetic-tetragonal liquid line to present the same character. Indeed, a mean field analysis of a multilayered version

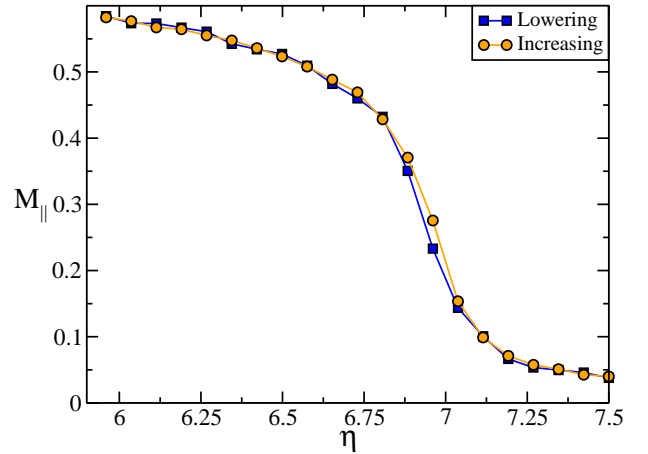


FIG. 11: (Color on line) $M_{||}$ as a function of η for a fixed Temperature $T = 1.3$.

of the model²² predicts first order SRT in the monolayer limit. The previous analysis seem to indicate that a different nature of the phase transition to the left and right of the maximum is possible, although more detailed studies are necessary in order to elucidate this point.

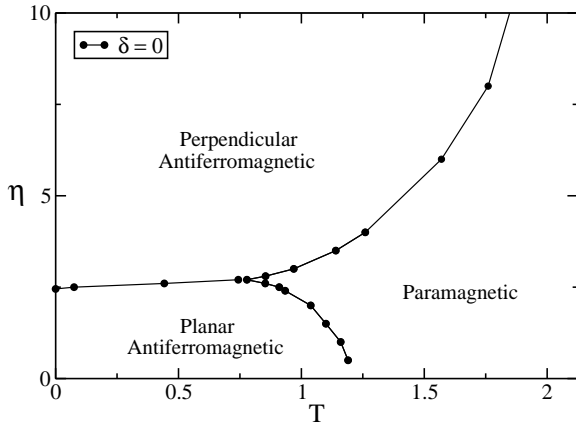


FIG. 12: Phase diagram for $\delta = 0$ (pure dipolar plus anisotropy)

IV. PURE DIPOLAR PLUS ANISOTROPY FILM

In this section we briefly discuss results for the limit where exchange interactions are absent, $\delta = 0$. Experimentally this limit may be relevant for the behavior of arrays of magnetic monodomain particles for application in data storage devices. Usually these arrays can be considered as composed of noninteracting dots, but as the density of dots grows dipolar effects may begin to be relevant for the magnetic behavior. Although relaxation effects of arrays of this type have been studied by several authors, much less is known on the thermodynamic properties of the system. In particular, MacIsaac *et al.*¹⁶ obtained a phase diagram by Monte Carlo simulations. Without exchange interactions the relevant ordered phases in this case are all antiferromagnetic: one out of plane, with sublattice magnetization and the other one in-plane^{16,17}. A SRT is also found in this limit, from a planar antiferromagnetic phase at small anisotropies to a perpendicular antiferromagnetic phase at large anisotropies. Similar to what happened in the $\delta \neq 0$ case, MacIsaac *et al.* also found a reverse order of appearance of the phases through the SRT with temperature (see figure 1 of Ref.¹⁶). We obtained instead a different behavior, again similar to the trend of the $\delta \neq 0$ case, from perpendicular at low temperatures to planar at high temperatures, as shown in figure 12.

Comparing with figure 1 we can note that the slope of the SRT line is very small. Nevertheless there is a finite window where the transition from out of plane sublattice magnetization to in-plane is sharp as can be seen in figure 13. Another important difference between the phase diagrams of figures 1 and 12 is the absence of the gap for any fixed anisotropy in the latter case. This may be related with the different symmetry of the phases in the pure dipolar case. Now there is no tetragonal phase and for large anisotropies the system goes directly from a perpendicular antiferromagnetic phase to a perpendicularly disordered phase with full rotational symmetry. In this sense the paramagnetic phase shows the same symmetry along the whole planar-paramagnetic line at variance with the corresponding line in the ferromagnetic case.

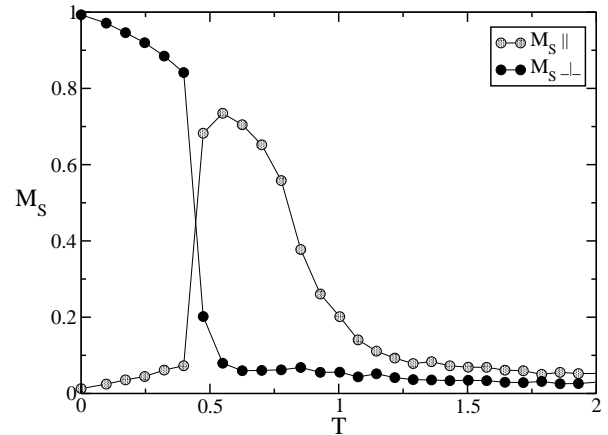


FIG. 13: Order parameters as function of temperature for $\delta = 0$ and $\eta = 2.6$. Here the system size is $L = 32$.

V. CONCLUSIONS

In this work we have analyzed the finite temperature phase diagram of a model for ultrathin ferromagnetic films with exchange, dipolar and perpendicular anisotropy interactions for two different values of the exchange constant (relative to the dipolar one). Particular emphasis was put in the $\delta = 3$ case, where the system presents a striped phase of width $h = 4$ at low temperatures and a SRT to a planar ferromagnetic phase as the temperature increases. Although we were not able to simulate systems with larger (and more realistic) values of the exchange constant, the overall qualitative good agreement with many experimental results indicates that the same global behavior should be expected. In particular, the comparison between our phase diagram and the temperature *vs.* film thickness of Won *et al.* for Fe/Ni/Cu films⁵ suggests that the film thickness acts as an effective inverse anisotropy. We also reproduced the gap between the striped and the planar phases found by those authors. Moreover, our results indicate that the physical origin of the gap relies in the presence of a fast-moving perpendicularly-oriented labyrinthine (tetragonal liquid) phase. Evidence of a similar phenomenon (a fast moving striped phase close to the order-disorder transition) in Fe on Cu films has been reported by Portmann *et al.*²³.

Concerning the thermodynamical nature of the different transitions involved in the phase diagram, we obtained a clear numerical evidence of a first order stripe-planar SRT at low temperatures. We also found evidence pointing toward a first order nature of the stripe-tetragonal liquid transition, consistent with previous results in the Ising (i.e., high anisotropy) limit^{8,9}.

The planar ferromagnet-disordered transition line presents a maximum in the (η, T) space. In the left part of this line, the disordered state is a tetragonal liquid state, while in the right part we have a transition to an isotropic paramagnetic state; above the maximum the system passes continuously (i.e., without any thermodynamical phase transition) from the tetragonal liquid to the paramagnet. This fact, together with

several other physical arguments, suggests the possibility of a change in the order of the transition around the maximum of the line, being weakly first order in the left part of the line and second order in the right part. If confirmed, this would imply the existence of a tricritical point around the maximum and a triple point where the three phases (stripe-planar-tetragonal) coexist. However, strong finite size effects did not allow us to give a definite answer concerning this point and further studies should be needed.

In the case of $\delta = 0$ we showed the existence of a SRT from

a perpendicular antiferromagnetic phase at low temperature to an in-plane antiferromagnetic phase at higher temperatures, at variance with previous reported results. The present results suggest that a SRT from a low temperature out-of plane to an in-plane phase at higher temperatures for low values of η is present for any value of δ .

This work was partially supported by grants from CONICET (Argentina), SeCyT, Universidad Nacional de Córdoba (Argentina), CNPq (Brazil), FONCyT grant PICT-2005 33305 (Argentina) and ICTP grant NET-61 (Italy).

* Electronic address: carubell@famaf.unc.edu.ar

† Electronic address: billoni@famaf.unc.edu.ar

‡ Electronic address: spighin@famaf.unc.edu.ar

§ Electronic address: cannas@famaf.unc.edu.ar

¶ Electronic address: stariolo@if.ufrgs.br

** Electronic address: tamarit@famaf.unc.edu.ar

†† Member of CONICET, Argentina

‡‡ Research Associate of the Abdus Salam International Centre for Theoretical Physics, Trieste, Italy

¹ O. Portmann, *Micromagnetism in the Ultrathin Limit* (Logos Verlag, ADDRESS, 2006).

² D. P. Pappas, K. P. Kamper, and H. Hopster, Phys. Rev. Lett. **64**, 3179 (1990).

³ R. Allenspach and A. Bischof, Phys. Rev. Lett. **69**, 3385 (1992).

⁴ Y. Yafet and E. M. Gyorgy, Phys. Rev. B **38**, 9145 (1988).

⁵ C. Won *et al.*, Phys. Rev. B **71**, 224429 (2005).

⁶ A. Vaterlaus *et al.*, Phys. Rev. Lett. **84**, 2247 (2000).

⁷ A. B. MacIsaac, J. P. Whitehead, M. C. Robinson, and K. De'Bell, Phys. Rev. B **51**, 16033 (1995).

⁸ S. A. Cannas, D. A. Stariolo, and F. A. Tamarit, Phys. Rev. B **69**, 092409 (2004).

⁹ S. A. Cannas, M. F. Michelon, D. A. Stariolo, and F. A. Tamarit, Phys. Rev. B **73**, 184425 (2006).

¹⁰ E. Rastelli, S. Regina, and A. Tassi, Phys. Rev. B **73**, 144418 (2006).

¹¹ A. B. MacIsaac, K. De'Bell, and J. P. Whitehead, Phys. Rev. Lett. **80**, 616 (1998).

¹² L. Nicolao and D. A. Stariolo, Physical Review B (Condensed Matter and Materials Physics) **76**, 054453 (2007).

¹³ D. G. Barci and D. A. Stariolo, Physical Review Letters **98**, 200604 (2007).

¹⁴ A. Abanov, V. Kalatsky, V. L. Pokrovsky, and W. M. Saslow, Phys. Rev. B **51**, 1023 (1995).

¹⁵ I. Booth, A. B. MacIsaac, J. P. Whitehead, and K. De'Bell, Phys. Rev. Lett. **75**, 950 (1995).

¹⁶ A. B. MacIsaac, J. P. Whitehead, K. De'Bell, and P. H. Poole, Phys. Rev. Lett. **77**, 739 (1996).

¹⁷ K. De'Bell, A. B. MacIsaac, I. N. Booth, and J. P. Whitehead, Phys. Rev. B **55**, 15108 (1997).

¹⁸ S. A. Pighin and S. A. Cannas, Physical Review B (Condensed Matter and Materials Physics) **75**, 224433 (2007).

¹⁹ D. Pescia and V. L. Pokrovsky, Phys. Rev. Lett. **65**, 2599 (1990).

²⁰ P. Politi, A. Rettori, and M. G. Pini, Phys. Rev. Lett. **70**, 1183 (1993).

²¹ P. Politi, Comments Cond. Matter Phys. **18**, 191 (1998).

²² A. Moschel and K. D. Usadel, Phys. Rev. B **51**, 16111 (1995).

²³ O. Portmann, A. Vaterlaus, and D. Pescia, Phys. Rev. Lett. **96**, 047212 (2006).